Nuclear Inst. and Methods in Physics Research, A 927 (2019) 396–400

Contents lists available at ScienceDirect

Nuclear Inst. and Methods in Physics Research, A

journal homepage: www.elsevier.com/locate/nima

Timing performance study of Multigap Resistive Plate Chamber with different gap size

Z. Liu [a,b,c,*], F. Carnesecchi [d,e], M.C.S. Williams [b,d,f], A. Zichichi [b,d,e], R. Zuyeuski [c,e]

[a] School of Nuclear Science and Technology, University of South China, Hengyang, China
[b] European Centre for Nuclear Research (CERN), Geneva, Switzerland
[c] ICSC World Laboratory, Geneva, Switzerland
[d] INFN and Dipartimento di Fisica e Astronomia, University of Bologna, Italy
[e] Museo Storico della Fisica e Centro Studi e Ricerche E.Fermi,Roma, Italy
[f] Gangneung-Wonju National University, Gangneung, South Korea

A R T I C L E I N F O

Keywords:
Multigap Resistive Plate Chamber
Gap size
Efficiency
Time resolution
Rate capability

A B S T R A C T

This paper reports on the results of time resolution measurements of Multigap Resistive Plate Chamber (MRPC). Three 20 gas gaps MRPCs were built with thin float glass sheets and different gap sizes: 160 μm, 140 μm and 120 μm. These chambers have been tested using a different gas flow configurations. The measurements indicate that to reach a better time resolution for small gap size (140 μm and 120 μm), a smaller gas volume of the chamber is preferable. The efficiency of the chambers in both gas flow configurations has been tested. A time resolution of 25 ps comprehensive of the front-end electronics jitter, with an efficiency of 98% has been achieved for the MRPC with 140 μm gas gaps; this is the best time resolution. Moreover, all the chambers have been tested for different particle flux. At the highest particle flux tested, a time resolution better than 60 ps together with an efficiency higher than 80% has been achieved for all the detectors at an instantaneous particle flux of 30 kHz/cm^2. From the efficiency and time resolution study, the rate capability for these three MRPC is similar.

1. Introduction

The Multigap Resistive Plate Chamber (MRPC) is a gaseous detector consisting of a stack of resistive plates [1]. Its good timing characteristics and low cost make it widely used as a Time of Flight (TOF) detector in nuclear and particle physics experiments [2] such as the ALICE experiment [3], STAR experiment [4] and HADES experiment [5]. With the higher pile-up of the next generation hadron colliders, such as the High Luminosity Large Hadron Collider (HL-LHC) [6] and the Future Circular Collider (FCC) [7], the requirement of a time resolution of a few tens of picoseconds becomes necessary; indeed such time resolution, added to the spatial information, would permit 4-D tracking, with the benefit, such as the assignment of tracks to vertices even at the future harsh environment. Building an MRPC with a time resolution better than 20 ps while maintaining an efficiency close to 100%, is possible, as reported in [8]. The main goal of our R&D is to design and build an MRPC with similar performance. but maintaining the feasibility of a large scale detector together with low cost and ease of construction, while minimising the material budget. Starting from the idea of [9], a deeper study has been performed based on the changing of the thickness of the MRPC gas gaps.

Another fundamental MRPC parameter is the rate capability; for example at the future Compressed Baryonic Matter (CBM) experiment at Facility for Antiproton and Ion Research (FAIR) [10], the TOF detectors are required to work with a continuous particle flux in the order of 1–10 kHz/cm^2 for the outer region and 10–25 kHz/cm^2 for the central region [11]. Thus the rate capability is a key characteristic for the MRPCs used at the CBM experiment. To improve the rate capability of the MRPC some methods have been tried: such as using materials with lower bulk resistivity [12], using resistive plates with thinner thickness [13], and reducing of gap size of MRPC [14]. In [9] we reported the rate capability of a 20-gap MRPC compared to a 6-gap MRPC (with the 6-gap MRPC having larger gap size). Also for this reason, this study of the gas gap thickness has been performed; a thinner design can simultaneously improve both the time resolution and enhance the rate capability. Three 20 gas gap MRPCs with a gap size of 160 μm, 140 μm, and 120 μm have been built and tested to study the effect of gap size for the time resolution and rate capability. These detectors have also been tested using a different gas flow design; the results of their efficiency, time resolution and rate capability are reported in this paper.

* Corresponding author at: European Centre for Nuclear Research (CERN), Geneva, Switzerland.
E-mail address: zheng.liu@cern.ch (Z. Liu).

https://doi.org/10.1016/j.nima.2019.02.068
Received 25 February 2019; Accepted 26 February 2019
Available online 28 February 2019

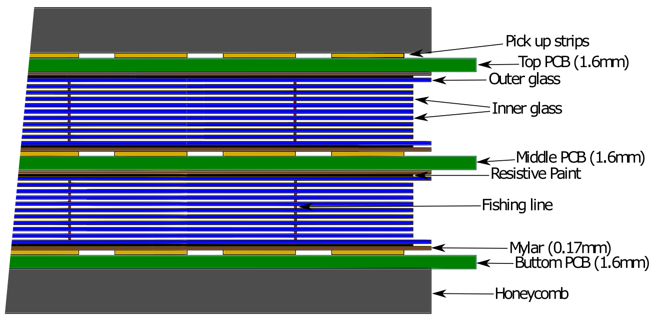

Fig. 1. Cross section of the double stack 20-gap MRPC.

2. MRPC construction

Following the MRPC configuration described in [9], three 20-gap MRPCs were constructed with the same structure but with different gap sizes. The gap sizes of these three MRPCs are 160 μm (160 μm-MRPC), 140 μm (140 μm-MRPC) and 120 μm (120 μm-MRPC). The schematic of cross section of the three MRPCs is shown in Fig. 1. They all have double stack configuration. Each stack is made with 2 outer glass plates and 9 inner glass plates. The external glass plates have a dimension of 22×22 cm^2; an 18×18 cm^2 area of the external glass sheet outer surface has been painted with resistive coating to form an electrode with a surface resistivity of 5 MΩ/□. The inner glass plates have a dimension of 18×18 cm^2. All glass plates are 0.28 mm thick and have a bulk resistivity of 1.3×10^{12} Ωcm at 24 °C. The spacers between the glass sheets are mono-filament commercial nylon fishing lines of different diameters (gas gap thickness): 160 μm, 140 μm and 120 μm. A mylar sheet was placed between the voltage electrode and the printed circuit board (PCB) to isolate the high voltage. Three PCBs with pick-up strips are used to read out the signals from the MRPC. The two resistive electrodes next to the middle PCB were connected with negative high voltage and the other two electrodes on the top and bottom layer connected to positive high voltage. Thus the MRPC has two anode pick-up strip planes (top and bottom) and one cathode pick-up strip plane (middle). The two anode strip planes are connected thus adding the signals of the two stacks together. The width of the pick-up strip is 1 cm on a pitch of 1.1 cm. The length of the strip is 21 cm. Two honeycomb panels are attached to the top and bottom layer of MRPC for mechanical support.

The three MRPCs have been mounted inside a gas-tight aluminium box; two different configurations for the gas flow have been studied (configuration A and B), involving different gas volumes.

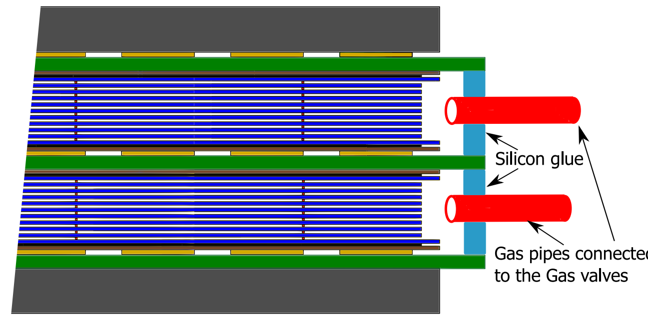

Fig. 3. Cross section of the MRPCs with gas sealing.

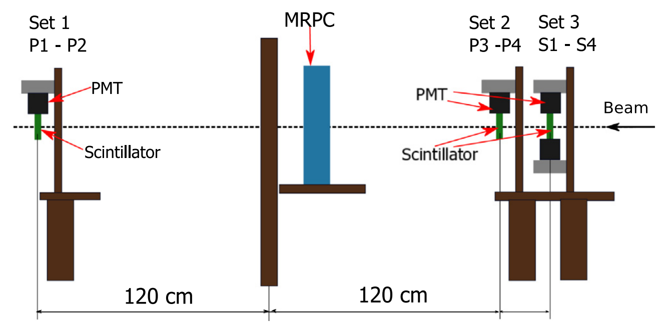

Fig. 4. The experiment setup for the MRPC test at the T10 test beam facility.

2.1. Gas flow configuration A

The configuration A, involves a large volume of gas; as shown in Fig. 2, the gas flows from the gas inlet of the box, and exits on the opposite of the box. The gas volume of box is $40 \times 27 \times 5$ cm^3.

2.2. Gas flow configuration B

In the configuration B the gas volume of the MRPC is largely reduced. The gas flow volume of MRPC is reduced by sealing the edge of the PCBs by silicon glue (CAF 4). Gas tubes are placed close to the edge of the glass and connected to the gas inlet. Gas tubes for exhaust are placed on the other side of MRPC and connected to the gas outlet. The silicon is placed between the PCBs as shown in Fig. 2. From the top view of the MRPC. the four sides of the MRPC are sealed as shown in Fig. 3. The gas volume of MRPC in configuration B is much smaller than configuration A. Taking the 160 μm-MRPC for example, the volume is about 22×22×20×0.016 cm^3 (coincident with the MRPC active volume), which is about 50 times smaller than the gas volume with configuration A.

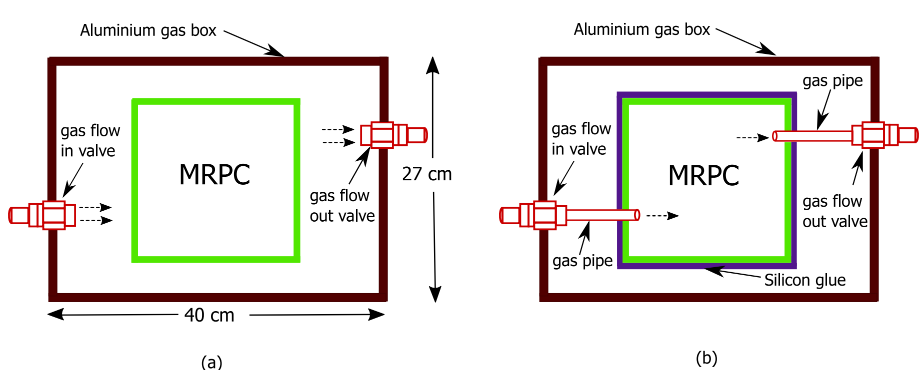

Fig. 2. The gas flow schematic of two gas configuration. (a) the gas configuration A. (b) the gas configuration B.

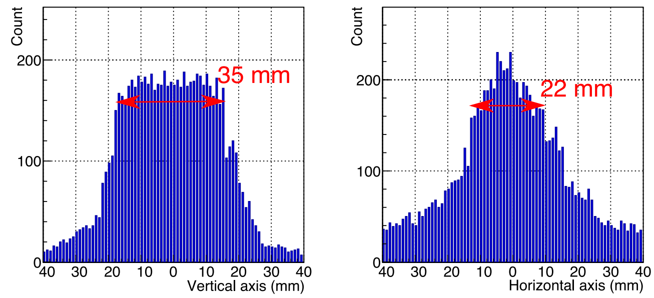

Fig. 5. The wire chamber profile in vertical and horizontal axis at the flux of 30 kHz/cm^2.

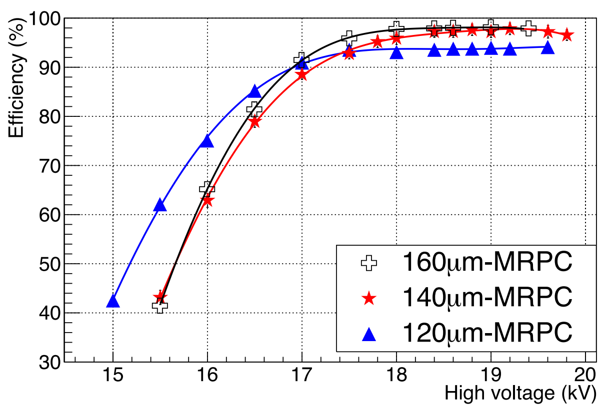

Fig. 6. The efficiency of the three MRPCs as a function of voltage at 2.5 kHz/cm^2. The lines are to guide the eye.

3. Experimental setup

All tests for the three MRPCs were completed in T10 test beam facility at CERN [15]. The experimental setup is shown in Fig. 4. The beam was mainly composed of negative pions with 5 GeV/c momentum and had a direction perpendicular to the chamber. A gas mixture of 95% $C_2H_2F_4$ and 5% SF_6 was distributed to the chambers with a flow rate of 5 l/h. All sets of scintillators were aligned with respect to the beam line; the logic AND of signals from the scintillator sets creates the trigger signal. Scintillator set 1 and set 2 define an area of the beam of 1.2×1.2 cm^2, which allows us to select a small (1.2×1.2 cm^2) area of the beam to study. Scintillator set 3 consists of two orthogonal scintillator bars with a dimension of $2 \times 2 \times 20$ cm^3. Both end of each bar is coupled to a PMT (S1 and S2 for one bar, S3 and S4 for the other bar). The average of the hit times of these four PMTs (S1–S4) is used as a time reference and gives a time resolution of 35.0 ± 0.7 ps as in [12]. The beam spill has a duration of 360 ms. By measuring the number of coincidences of set 1 and set 2 during the spill we can monitor the instantaneous flux of particles that go through the MRPCs. The beam size is measured by a wire chamber. Fig. 5 shows the wire chamber profile in both the vertical axis and horizontal axis at the flux of 30 kHz/cm^2. As can be seen from the wire chamber, the beam is focused on a cross section of 22 mm × 35 mm. Within this spot area, the intensity is constant. Thus in the small area (1.2 × 1.2 cm^2), the MRPC is illuminated uniformly with particles during the 360 ms spill. The MRPCs were mounted on an X–Y moving table between PMT Set 1 and Set 2. The beam was centred in the middle of one pick up strip of the MRPC by adjusting the position of the table. The signals from the MRPC are discriminated by the NINO ASIC [16] and readout by WaveCatcher [17].

Table 1
The parameters of the three MRPCs.

	160 μm-MRPC	140 μm-MRPC	120 μm-MRPC
Total gap thickness of a stack	1.6 mm	1.4 mm	1.2 mm
HV at the start of plateau	18 kV	18.4 kV	17.5 kV
Electric field	112.5 kV/cm	131.4 kV/cm	145.8 kV/cm

4. Results and discussion

4.1. Performance of MRPCs at different voltages

The three MRPCs with two different gas volumes have been first tested at an instantaneous particle flux of 2.5 kHz/cm^2. In both gas flow configurations, the efficiency curve of each MRPC has similar values. The efficiency of the three MRPCs with a small gas volume is shown in Fig. 6. The efficiency plateau of 160 μm-MRPC and 140 μm-MRPC are similar and all reach 98%. For the 120 μm-MRPC an efficiency plateau of 94% is reached earlier (17.5 kV) compared to the other two MRPCs. As shown in Table 1, a higher electric field is needed to compensate the thinner gap size of the MRPC. However, the very high electric field needed for the 120 μm-MRPC also increases the percentage of streamer production can be seen from in Fig. 7. There is another ToT peak between 18 ns and 30 ns for 120 μm-MRPC ToT distribution. When operating the MRPCs on the efficiency plateaus, the dark current of the 160 μm-MRPC and the 140 μm-MRPC are in the range between 30 nA and 60 nA. The dark current of the 120 μm-MRPC is higher and in the range between 40 nA to 100 nA. There is little difference of the dark current for the two gas configurations.

The time that the particle traversed the MRPC was determined from the average of the time measured at each end of the strip, thus the measured MRPC time is independent of the position of the hit. The time measurements have been corrected for the time slewing effect; this was necessary since the NINO chip is a fixed threshold discriminator. More details on this effect are reported in [9]. The time difference between the 140 μm-MRPC and the reference time obtained from PMTs (S1–S4) after correction has a sigma of 43.0 ± 0.8 ps at 18.4 kV (see Fig. 8). A time resolution of 25.0 ± 1.1 ps is obtained by subtracting the jitter of reference time in quadrature. Following the same procedure, the time resolution of the three MRPCs at different voltages and gas volume are obtained and shown in Figs. 9 and 10, Fig. 9 for gas configuration A and Fig. 10 for gas configuration B. The time resolution of MRPCs varies with different applied voltages. Comparing the different gas volume, the best time resolution for the 160 μm-MRPC is 31 ps, obtained in both gas volumes. The time resolution for the 140 μm-MRPC and 120 μm-MRPC have significantly better time resolution for the small gas volume (configuration B) than the large gas volume (configuration A). For the small gas volume, the 140 μm-MRPC reached a time resolution of 25 ps, better than the 27 ps of 120 μm-MRPC and the 31 ps of 160 μm-MRPC. We expected better time resolution as the gap size decreases. As seen from Fig. 10 the 120 μm-MRPC does not give better time resolution than that of the 140 μm-MRPC. Another interesting point of the result is that the best time resolution for 140 μm-MRPC and 120 μm-MRPC are obtained in the small gas volume. It could be related to the gas flow; for the 140 μm-MRPC and 120 μm-MRPC, the gap size is quite small, thus a faster gas supply is needed for refresh the polluted gas. The small volume ensure that the gas refreshment are fast enough thus the MRPC can operate in a good condition and provide better timing. This gas pollution effect has also been observed in the muon telescope detector in RHIC-STAR [18]. The performance of MRPC degrades with big gas volume. It also can be seen in Fig. 10, the time resolution of 160 μm-MRPC is below 32 ps from 18.8 kV to 19.6 kV. The 140 μm-MRPC have a time resolution better than 26 ps from 18.6 kV to 19.6 kV. The time resolution of 120 μm-MRPC is below 28 ps from 18.4 kV to 19.6 kV. The three MRPCs have a long efficiency plateau and also a wide voltage range reaching excellent time resolution.

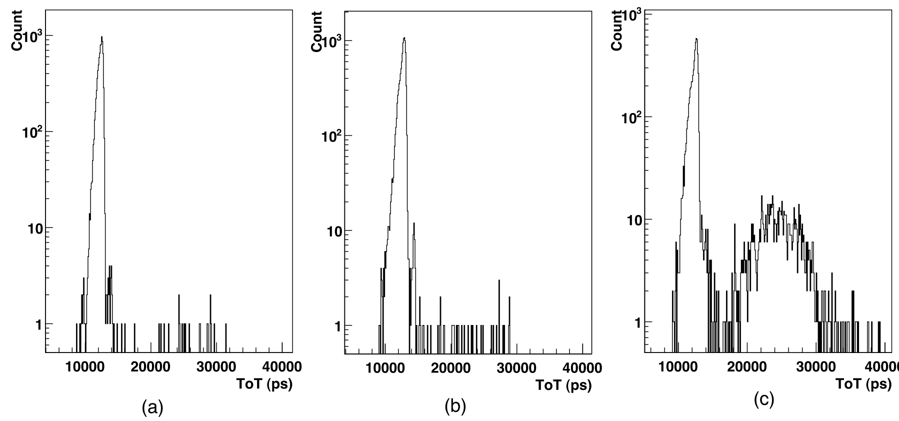

Fig. 7. The time over threshold (ToT) distribution of three MRPCs at 18.4 kV. (a) 160 μm-MRPC. (b) 140 μm-MRPC. (c) 120 μm-MRPC.

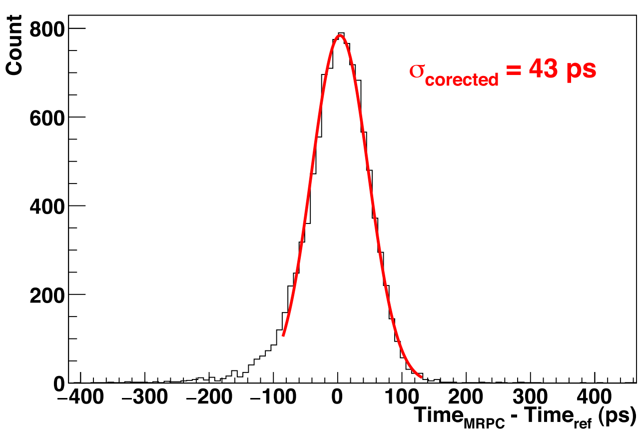

Fig. 8. Time difference between time reference PMTs (S1–S4) and 140 μm-MRPC after slewing corrections. The applied voltage is 18.8 kV.

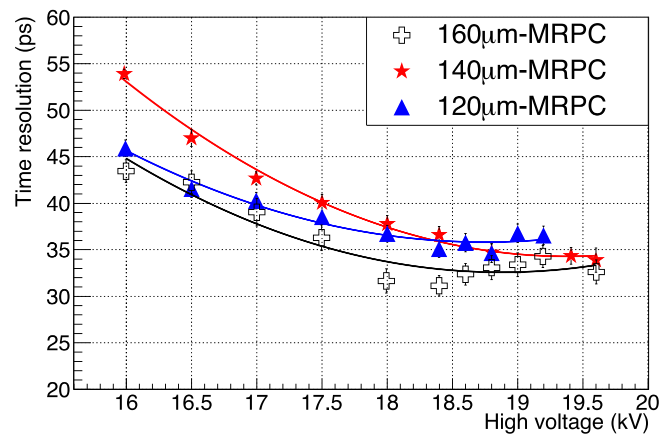

Fig. 9. The time resolution of the three MRPCs as a function of voltage at 2.5 kHz/cm^2 with large gas volume. The lines are to guide the eye.

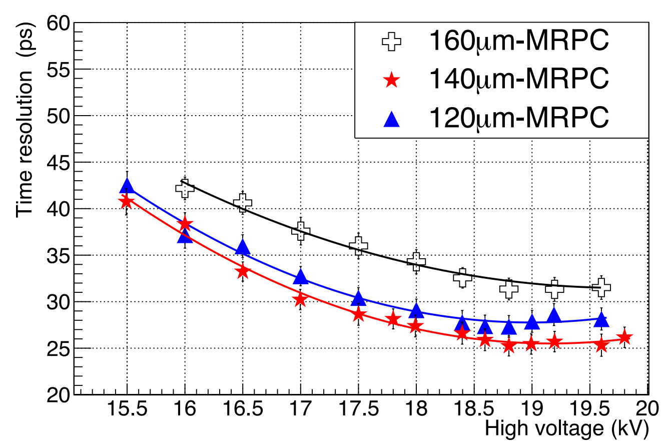

Fig. 10. The time resolution of the three MRPCs as a function of voltage at 2.5 kHz/cm^2 with small gas volume. The lines are to guide the eye.

4.2. The performance of MRPCs at different flux

As discussed previously, the three MRPCs show a high efficiency and excellent time resolution at the voltage of 18.8 kV; this value has been chosen for the rate capabilities study. Since better time resolutions have been obtained with the small gas volume configuration, we choose this gas flow configuration for the high flux test. In this paper, the relative performance of the three chambers is compared for the same instantaneous flux condition. However, for the rate capability measurement, it is important to point out that spot illumination with a pulsed beam was used; this situation is different from a flood illumination with a continuous flux of particle.

To test the rate capability of the MRPCs at high particle flux, we increased the instantaneous flux of particles up to 30.0 kHz/cm^2 during the beam spill. The beam spill has a period of 360 ms; the time between each spill is 10–20 s depending on the PS operation. Thus the MRPC has a long time to recover between the spills. As pointed out in [9], the efficiency of the MRPCs decreases during the first half of the spill period while it is relatively stable for the last 100 ms. Thus, to make the result closer to the continuous flux condition, we used the data obtained during the last 100 ms of the spill. The efficiency of the three MRPCs as a function at different flux is shown in Fig. 11. It can be noticed that the efficiency at different flux of the 160 μm-MRPC and 140 μm-MRPC are quite similar. The efficiencies of the 160 μm-MRPC, 140 μm-MRPC and 120 μm-MRPC at an instantaneous flux of 30 kHz/cm^2 reduce to 82%, 80%, and 83%, respectively.

To obtain the time resolution of the MRPCs in a condition equivalent to a continuous flux, we followed a similar strategy as for the efficiency, the data for only the last 100 ms of the spill are used to calculate the time resolution. Fig. 12 shows the time resolution of MRPCs as function of flux. As can be seen, the time resolution of all MRPCs deteriorate at higher flux.

4.3. Summary

The three 20-gap MRPCs with different gap size have been tested in the T10 test beam. For the very thin gap size MRPC, the small

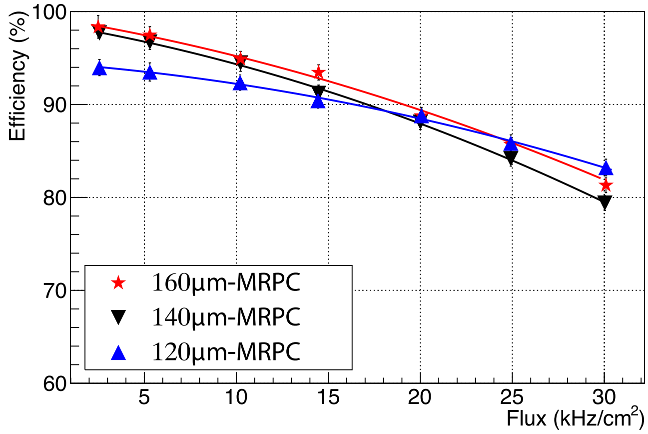

Fig. 11. The efficiency of the three MRPCs as a function at different flux by using only the data at the last 100 ms of the spill. The high voltage of the three MRPCs is fixed at 18.8 kV.

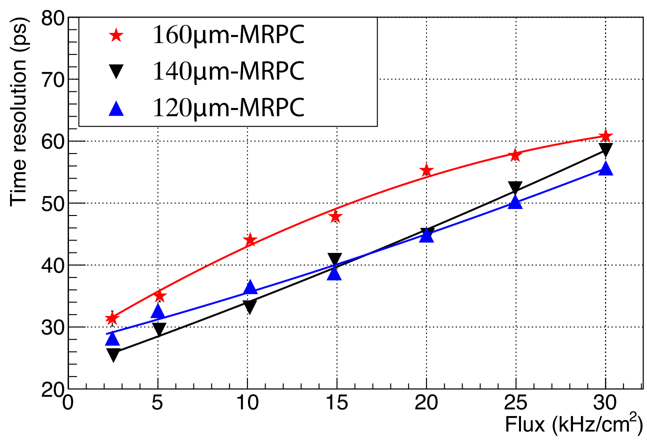

Fig. 12. The time resolution of the three MRPCs as a function of different flux. The high voltage of the three MRPCs is fixed at 18.8 kV. Only the data at the last 100 ms of the spill are used.

volume configuration gives better timing performance. Among the three MRPCs, the 140 μm-MRPC gives the best time resolution of 25 ps. For their rate capability, we do not find a significant difference. So for the 20-gap double stack configuration MRPC, the 140 μm gap size is optimal for the application of precision timing measurement at high flux.

Acknowledgements

The results presented here were obtained at the T10 test beam in the east hall at CERN. The authors acknowledge the support received by the operators of the PS.

References

[1] E. Cerron Zeballos, et al., A new type of resistive plate chamber: the multigap RPC, Nucl. Instrum. Methods Phys. Res. A 374 (1) (1996) 132–135.

[2] A. Akindinov, et al., The multigap resistive plate chamber as a time-of-flight detector, Nucl. Instrum. Methods Phys. Res. A 456 (1) (2000) 16–22.

[3] A.N. Akindinov, et al., Latest results on the performance of the multigap resistive plate chamber used for the ALICE TOF, Nucl. Instrum. Methods Phys. Res. A 533 (1) (2004) 74–78.

[4] W.J. Llope, S.T.A.R. Collaboration, Star collaboration multigap rpcs in the star experiment at rhic, Nucl. Instrum. Methods Phys. Res. A 661 (2012) S110–S113.

[5] D. Belver, et al., The HADES RPC inner TOF wall, Nucl. Instrum. Methods Phys. Res. A 602 (2009) 687–690.

[6] G. Apollinari, et al. (Eds.), High-Luminosity Large Hadron Collider (HL-LHC): Preliminary Design Report, CERN-2015-005, CERN, Geneva Switzerland, 2015.

[7] M. Benedikt, F. Zimmermann, Future circular colliders, in: Proceedings of the International School of Physics. Enrico Fermi, vol. 194, IOS Press; SIF, 2016, pp. 73–80.

[8] S. An, et al., A 20 ps timing device - A Multigap Resistive Plate Chamber with 24 gas gaps, Nucl. Instrum. Methods Phys. Res. A 594 (1) (2008) 39–43.

[9] Z. Liu, et al., 20 gas gaps multigap resistive plate chamber: Improved rate capability with excellent time resolution, Nucl. Instrum. Methods Phys. Res. A 908 (2018) 383–387.

[10] Johann M. Heuser, The compressed baryonic matter experiment at FAIR, in: EPJ Web of Conferences, vol. 13, EDP Sciences, 2011.

[11] I. Deppner, et al., The CBM Time-of-Flight wall: a conceptual design, J. Instrum. 9 (10) (2014) C10014.

[12] Wang Jingbo, et al., Development of multi-gap resistive plate chambers with low-resistive silicate glass electrodes for operation at high particle fluxes and large transported charges, Nucl. Instrum. Methods Phys. Res. A 621 (1–3) (2010) 151–156.

[13] Zhu Weiping, et al., A thin float glass MRPC for the outer region of CBM- TOF wall, Nucl. Instrum. Methods Phys. Res. A 735 (2014) 277.

[14] K.S. Lee, et al., J. Instrument (2012) P10009.

[15] http://sba.web.cern.ch/sba/BeamsAndAreas/East/East.htm.

[16] F. Anghinolfi, et al., NINO: an ultra-fast and low-power front-end amplifier/discriminator ASIC designed for the multigap resistive plate chamber, Nucl. Instrum. Methods Phys. Res. A 533 (1) (2004) 183–187.

[17] D. Breton, J. Maalmi, E. Delagnes, Using ultra fast analog memories for fast photo-detector read out, in: NDIP 2011, Lyon.

[18] P. Lyu, et al., Gas related effects on multigap RPC performance in high luminosity experiments, J. Instrum. 11 (2016) C11041.